Metallocyclopeptide Complexes with $M^{II}(S{\cdot}Cys)_4$ Chromophores

Alexander L. Nivorozhkin,[†] Brent M. Segal,[†] Kristin B. Musgrave,[§] Steven A. Kates,[‡] Britt Hedman,*[,§] Keith O. Hodgson,*[,§] and R. H. Holm*[,†]

Department of Chemistry and Chemical Biology, Harvard University, Cambridge, Massachusetts 02138, PE Biosystems, Framingham, Massachusetts 01701, and Department of Chemistry, Stanford University and Stanford Synchrotron Radiation Laboratory, SLAC, Stanford, California 94305

Received April 16, 1999

The tetracysteinyl peptide *cyclo*[Lys[1,12]](Gln-Cys-Gly-Val-Cys-Gly-Lys-Cys-Ile-Ala-Cys-Lys) ($\subset L(Cys{\cdot}SH)_4$) was synthesized by solid-phase methods using an Fmoc/*t*-Bu/allyl strategy on a PAL−PEG−PS support. The formation of the 1:1 complexes with M = Fe^{2+}, Co^{2+}, and Ni^{2+} was observed by spectrophotometric monitoring of reactions in aqueous solution at pH 7.5. Size exclusion chromatography indicated that the peptide is a monomer and the complexes are dimers $[M_2(\subset L(Cys{\cdot}S)_4)_2]$ in aqueous buffer at pH 7.5. Cobalt and nickel K-edge X-ray absorption data and EXAFS analysis of $[Co_2(\subset L(Cys{\cdot}S)_4)_2]$ and $[Ni_2(\subset L(Cys{\cdot}S)_4)_2]$ as lyophilized solids are reported. Derived bond distances are Co−S = 2.30 Å and Ni−S = 2.21 Å. From the collective results provided by absorption spectra, K-edges, EXAFS, and bond length comparisons with known structures, it is shown that $[Fe_2(\subset L(Cys{\cdot}S)_4)_2]$ and $[Co_2(\subset L(Cys{\cdot}S)_4)_2]$ possess distorted tetrahedral structures and $[Ni_2(\subset L(Cys{\cdot}S)_4)_2]$ has distorted square planar stereochemistry. The Co(II) chromophore is particularly distinctive of the assigned structure, displaying three components of the parent tetrahedral ligand field transition $^4A_2 \rightarrow {}^4T_1(P)$ (610, 685, 740 nm). The observed structures conform to the intrinsic stereochemical preferences of the metal ions. Structures for the binuclear complexes are suggested. These are the first characterized metal complexes of a cysteinyl cyclopeptide and among the few well-documented complexes of synthetic cyclopeptides. This study is a desirable first step in the design of cyclic peptides for the binding of mononuclear and polynuclear metal centers.

Introduction

Cyclic amino acid sequences constitute the elements of many biologically active compounds such as antibiotics and toxins. In recent years, cyclic peptides, with their attendant structural constraints, have been applied to a number of problems, including protein folding and drug design.[1−7] The metal-binding propensities of cyclic peptides and the properties of the resultant complexes, especially those containing cysteinyl residues, are largely unexplored.[8−11] This situation stands in contrast to the increasing use of functionalized de novo designed acyclic peptides to stabilize desired modes of metal ion coordination[12−14] and to the large number of M−S·Cys binding interactions in biology.[15−17] In addition, there is an abundance of nonpeptidic synthetic metal thiolate complexes which includes numerous polynuclear structural motifs.[18−20] We have initiated the synthesis of relatively small cysteinyl cyclopeptides and an examination of their binding properties toward individual metal ions and metal clusters. A goal of this work is the attainment of well-defined mononuclear and polynuclear coordination units related to those in proteins for structural and reactivity studies.

One immediate problem is the formation and stabilization of the mononuclear $Ni^{II}(S{\cdot}Cys)_4$ coordination unit. This unit is of interest in its own right, and may also act as a precursor of heterometallic bridged binuclear units, as in the $(Cys{\cdot}S)_2Ni(\mu\text{-}Cys{\cdot}S)_2Fe$ fragment of the catalytic sites of [NiFe]-hydrogenases.[21−23] Among synthetic complexes, monomeric tetrathiolates are confined to the distorted tetrahedral species $[Ni(SC_6H_4X)_4]^{2-}$ (X = H, Cl, Me), derived exclusively from arenethiolates.[24−27] Monomeric diamagnetic bis(alkyldithiolato)Ni(II) complexes have been prepared and their planar structures

[†] Harvard University.
[‡] PE Biosystems. Current address: Consensus Pharmaceuticals, Medford, MA.
[§] Stanford University and SSRL.

(1) Camarero, J. A.; Pavel, J.; Muir, T. W. *Angew. Chem., Int. Ed. Engl.* **1998**, *37*, 347.
(2) Haubner, R.; Finsinger, D.; Kessler, H. *Angew. Chem., Int. Ed. Engl.* **1997**, *36*, 1375.
(3) Rizo, J.; Gierasch, L. *Annu. Rev. Biochem.* **1992**, *61*, 387.
(4) Yamazaki, T.; Said-Nejad, O. E.; Schiller, P. W.; Goodman, M. *Biopolymers* **1991**, *31*, 887.
(5) Al-Obedi, F.; Castrucci, A. M. del L.; Hadley, M. E.; Hruby, V. J. *J. Med. Chem.* **1989**, *32*, 2555.
(6) Goldenberg, D. P. *J. Cell. Biochem.* **1985**, *29*, 321.
(7) Goldenberg, D. P.; Greighton, T. E. *J. Mol. Biol.* **1984**, *179*, 527.
(8) Haas, K.; Ponikwar, W.; Nöth, H.; Beck, W. *Angew. Chem., Int. Ed.* **1998**, *37*, 1086.
(9) Comba, P.; Cusack, R.; Fairlie, D. P.; Gahan, L. R.; Hanson, G. R.; Kazmaier, U.; Ramlow, A. *Inorg. Chem.* **1998**, *37*, 6721.
(10) Tuchscherer, G.; Lehmann, C.; Mathieu, M. *Angew. Chem., Int. Ed.* **1998**, *37*, 2990.
(11) For a recent example of metal binding to a cyclic cysteinyl peptide, cf.: Tanaka, K.; Shigemori, K.; Shionoya, M. *Chem. Commun.* **1999**, 2475.
(12) Regan, L. *Annu. Rev. Biophys. Biomol. Struct.* **1993**, *22*, 257.
(13) Regan, L. *Trends Biochem. Sci.* **1995**, *20*, 280.
(14) Gibney, B. R.; Rabanal, F.; Dutton, P. L. *Curr. Opin. Chem. Biol.* **1997**, *1*, 537.
(15) Holm, R. H.; Kennepohl, P.; Solomon, E. I. *Chem. Rev.* **1996**, *96*, 2239.
(16) Berg, J. M.; Shi, Y. *Science* **1996**, *271*, 1081.
(17) Beinert, H.; Holm, R. H.; Münck, E. *Science* **1997**, *277*, 653.
(18) Dance, I. G. *Polyhedron* **1986**, *5*, 1037.
(19) Blower, P. J.; Dilworth, J. R. *Coord. Chem. Rev.* **1987**, *76*, 121.
(20) Krebs, B.; Henkel, G. *Angew. Chem., Int. Ed. Engl.* **1991**, *30*, 769.
(21) Volbeda, A.; Charon, M.-H.; Piras, C.; Hatchikian, E. C.; Frey, M.; Fontecilla-Camps, J. C. *Nature* **1995**, *373*, 580.
(22) Volbeda, A.; Garsin, E.; Piras, C.; de Lacey, A. L.; Fernandez, V. M.; Hatchikian, E. C.; Frey, M.; Fontecilla-Camps, J. C. *J. Am. Chem. Soc.* **1996**, *118*, 12989.
(23) Higuchi, Y.; Yagi, T.; Yasuoka, N. *Structure* **1997**, *5*, 1671.

10.1021/ic990421l CCC: $19.00
Published on Web 05/02/2000

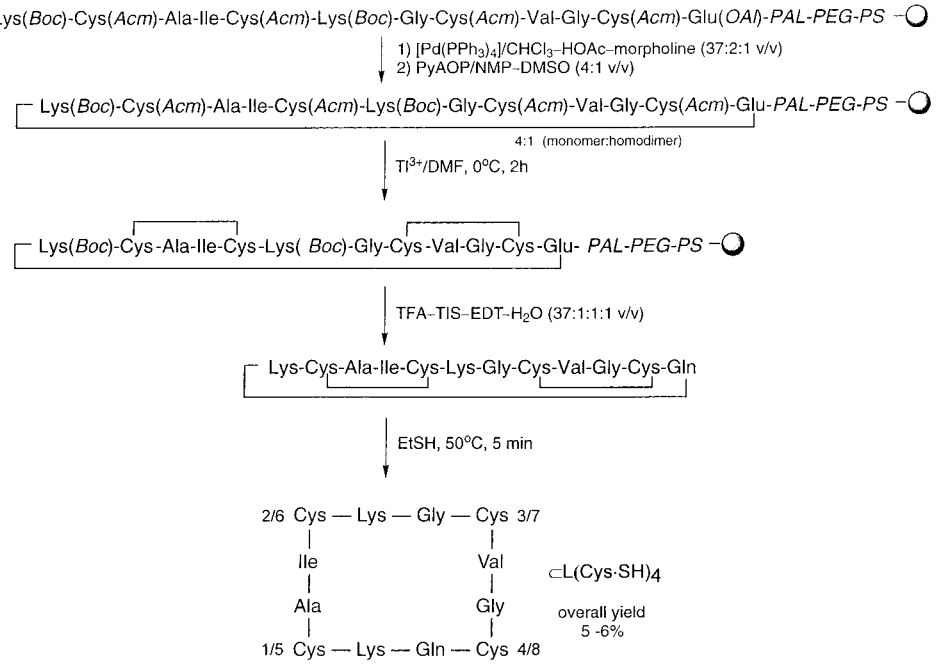

Figure 1. Scheme for the synthesis of *cyclo*[Lys[1,12]](Gln-Cys-Gly-Val-Cys-Gly-Lys-Cys-Ile-Ala-Cys-Lys) (⊂L(Cys·SH)$_4$) using an Fmoc/*t*-Bu/allyl strategy and including a Tl^{3+} protocol for Cys-Acm deprotection.

demonstrated by X-ray determinations.[28−30] However, certain of these tend to form polynuclear entities, especially in protic media.[28,31] At present, nickel(II)-substituted rubredoxin is the only known mononuclear alkylthiolate species $[Ni(SR)_4]^{2-}$.[32,33]

We have explored several generic design principles that could be applied to the preparation of cysteinyl cyclopeptides and their complexes with mononuclear and polynuclear metal centers. In the first phase of this work, the synthesis of a tetracysteinyl cyclopeptide and its Fe(II), Co(II), and Ni(II) complexes are described. The binding stoichiometry and molecularity of the complexes have been established, and the structures of the $M^{II}(S{\cdot}Cys)_4$ coordination units have been deduced from optical spectra and X-ray absorption spectroscopic measurements. Certain initial results have been reported.[34]

Experimental Section[35]

Materials. Reagents for peptide synthesis were purchased from PerSeptiveBiosystems. The compounds $Fe(OAc)_2$ (Strem) and $CoCl_2{\cdot}6H_2O$ and $NiCl_2{\cdot}6H_2O$ (Aldrich) were employed for generation of metallopeptide complexes.

Peptide Synthesis. Peptide construction of *cyclo*[Lys[1,12]](Gln-Cys-Gly-Val-Cys-Gly-Lys-Cys-Ile-Ala-Cys-Lys) (⊂L(Cys·SH)$_4$) was accomplished using an Fmoc/*t*-Bu/allyl strategy[36] on a PAL−PEG−PS support (0.175 mmol/g). The synthetic procedure is outlined in Figure 1. Key features for successful synthesis include side-chain anchoring Fmoc−Glu(OH)−OAl as opposed to the corresponding Asp derivative to prevent aspartamide formation, and Acm protection of the four Cys residues, which has been shown to increase the overall yield compared to trityl or S−Bu^t protection schemes. Two Lys residues were included to enhance solubility in water. Linear Cys(Acm)-protected peptide resins were assembled on a Pioneer peptide synthesizer via HATU/DIPEA based methods as described elsewhere.[37] In a typical preparation, 0.1 mmol of resin was treated under dinitrogen for 2 h with 0.5 g of [Pd(PPh$_3$)$_4$] in a 15 mL solution of $CHCl_3$−HOAc−morpholine (37:2:1 v/v) for allyl deprotection. The resin was washed alternately with 0.5% solutions (3 × 15 mL) of DIEA in DMF and sodium diethyldithiocarbamate in DMF, and subsequently washed with DMF, dichloromethane, and methanol (all 3 × 15 mL). The Fmoc was removed with 15 mL of 20% piperidine in DMF over 30 min. The resin was washed with 40 mL of 0.4% HCl in DMF to remove any excess piperidine and was dried briefly. The resin was slurried in 10 mL of NMP/DMSO (4:1 v/v) containing PyAOP (5 equiv) and DIEA (10 equiv). Dinitrogen was bubbled gently through the slurry for 16 h as the cyclic adduct was formed. Completion of the cyclization was monitored by means of the Kaiser test. The resin was washed with DMF, dichloromethane, and methanol (all 3 × 15 mL), slurried in 10 mL of DMF containing 0.25 mM $Tl(O_2CCF_3)_3$, and allowed to react at 0 °C for 90 min. The on-resin oxidation removes the Acm side-chain protecting group,

(24) Holah, D. G.; Coucouvanis, D. *J. Am. Chem. Soc.* **1975**, *97*, 6917.
(25) Swenson, D.; Baenziger, N. C.; Coucouvanis, D. *J. Am. Chem. Soc.* **1978**, *100*, 1932.
(26) Yamamura, T.; Miyame, H.; Katayama, Y.; Sasaki, Y. *Chem. Lett.* **1985**, 269.
(27) Rosenfield, S. G.; Armstrong, W. H.; Mascharak, P. K. *Inorg. Chem.* **1986**, *25*, 3014.
(28) Snyder, B. S.; Rao, Ch. P.; Holm, R. H. *Aust. J. Chem.* **1986**, *39*, 963.
(29) Baidya, N.; Marscharak, P. K.; Stephan, D. W.; Campagna, C. F. *Inorg. Chim. Acta* **1990**, *177*, 233.
(30) Fox, S.; Wang, Y.; Silver, A.; Millar, M. *J. Am. Chem. Soc.* **1990**, *112*, 3218.
(31) Leussing, D. L.; Alberts, G. S. *J. Am. Chem. Soc.* **1960**, *82*, 4458.
(32) Kowal, A. T.; Zambrano, I. C.; Moura, I.; Moura J. J. G.; Le Gall, J.; Johnson M. K. *Inorg. Chem.* **1988**, *27*, 1162.
(33) This statement excludes mononuclear Ni(II) complexes with unsaturated ligands such as dithiolenes, dithiooxalate, dithiosquarate, and dithiotropolonate.
(34) Nivorozhkin, A.; Kates, S. A.; Holm, R. H. In *Peptides 1998*; Bajkusz, S., Hudecz, F., Eds.; Akadémiai Kiadó: Budapest, 1999; pp. 522−523.
(35) *Abbreviations:* Acm, acetamidomethyl; DIEA, *N*,*N*-diisopropylethylamine; EDT, ethane-1,2-dithiol; ES, electrospray; HATU, *N*,*N*-[(dimethylamino)-1*H*-1,2,3-triazolo[4,5-*b*]pyridin-1-yl-methylene]-*N*-methylmethanaminium hexafluorophosphate *N*-oxide; HEPES, (*N*-[2-hydroxyethyl]piperazine-*N*′-ethane-sulfonic acid); NMP, *N*-methylpyrrolidone; PAL, 5-(4-(9-fluorenylmethyloxycarbonyl)aminomethyl-3,5-dimethoxyphenoxy)valeric acid handle; PEG−PS, poly(ethylene glycol)−polystyrene graft support; PyAOP, 7-azabenzotriazol-1-yl-oxytris-(pyrrolidino)phosphonium hexafluorophosphate; S_2-norborane, bicyclo-[2.2.1]heptane-*exo*, *cis*-2,3-dithiolate(2-); S_2-*o*-xyl, *o*-xylyl-α,α′-dithiolate(2−); TFA, trifluoroacetic acid; TIS, triisopropylsilane; XAS, X-ray absorption spectroscopy.
(36) Kates, S. A.; Sole, N. A.; Johnson, C. R.; Hudson, D.; Barany, G.; Albericio, F. *Tetrahedron Lett.* **1993**, *34*, 1549.
(37) Londo, T. R.; Kehoe, T.; Kates, S. A.; Hantman, S.; Gordon, N. F. *Lett. Peptide Sci.* **1998**, *5*, 285.

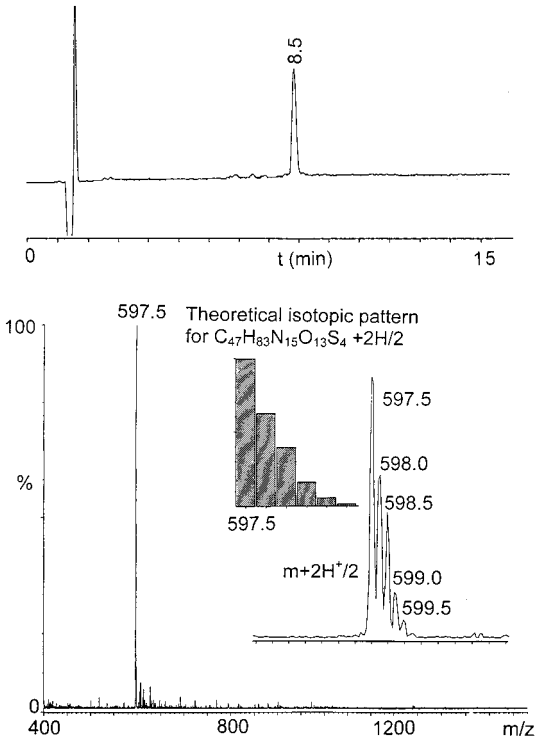

Figure 2. Analytical reversed-phase HPLC trace (upper) and ES−MS spectrum of purified cyclopeptide ⊂L(Cys·SH)$_4$ (lower). The observed and theoretical (M + 2H$^+$)/2 peak patterns of the fully reduced peptide are shown.

resulting in the corresponding bis-disulfide(s) (one possible product is shown in Figure 1). The resin was washed thoroughly with DMF and methanol and dried in vacuo overnight. Peptide cleavage from the resin was performed with 20 mL of TFA/EDT/TIS/H_2O (37:1:1:1 v/v) for 2 h. The resin was separated from the cleavage solution by filtration and washed with 10 mL of TFA. The combined filtrate and washings (ca. 30 mL) were concentrated in vacuo to ca. 3 mL, and the peptide was precipitated by addition of 50 mL of cold ether. The reaction mixture was maintained at −20 °C overnight. The crude peptide was separated by centrifugation and thoroughly washed with cold ether (3 × 50 mL). The white powder was dissolved in 5 mL of deionized filtered water and purified by reversed phase HPLC. Separations were performed with a Rainin Dynamax instrument equipped with YMC C_{18} analytical (120 Å, 100 × 4.6 mm) and preparative (120 Å, 100 × 20 mm) columns (Figure 2). Linear gradients of 0.1% TFA in acetonitrile and 0.1% aqueous TFA were run at 1 and 20 mL/min flow rate, respectively, from 1.5:8.5 to 3:7 v/v over 15 min with UV detection at 214 nm. Fractions were collected from preparative HPLC purification, combined, lyophilized, and redissolved in 2 mL of water containing 50 μL of ethanethiol. The solution was heated to 50 °C for 5 min, lyophilized, and the residue washed with hexane (3 × 50 mL) to eliminate disulfides formed by aerial oxidation during purification. The yield of purified peptide is 6 mg (5%). Oxidation by Tl^{3+} was found to be the yield-limiting step in the preparation. ES−MS: m/z^+ calculated for $C_{47}H_{83}N_{15}O_{13}S_4$, 1193; found, [M + H$^+$] 1194.0, [M +2H$^+$/2] 597.5 (Figure 2). ES−MS spectra were recorded on a Platform 2 mass spectrometer (Micromass Instruments, Danvers, MA). Amino acid analysis confirmed that all noncysteine residues are present in the proper stoichiometry.[38]

Complexation Reactions. These reactions were followed using a Cary model 3 or model 50 spectrophotometer under strictly anaerobic conditions. Solutions of cyclic peptide were prepared from 1 to 2 mg of lyophilized peptide in a known volume of water (2−4 mL). A 10 μL aliquot of the peptide solution was submitted for amino acid analysis at the Harvard Microchemistry Facility. After hydrolysis in 6 N HCl at 150 °C, samples were subjected to precolumn phenylisothiocyanate derivatization[38] using an ABI model 420A amino acid analyzer. The alanine mass determined was used to calculate the final peptide mass. The peptide solution was treated with 50 μL of ethanethiol and heated to 50 °C for 5 min. The peptide was isolated by lyophilization, washed with hexane, and dried in vacuo. Stock solutions of peptide were prepared in 20 mM HEPES buffer with 50 mM NaCl at pH 7.5. Titrations were performed by addition of ca. 2 μL aliquots of metal ion stock solutions in water to 1 mL of peptide solution.

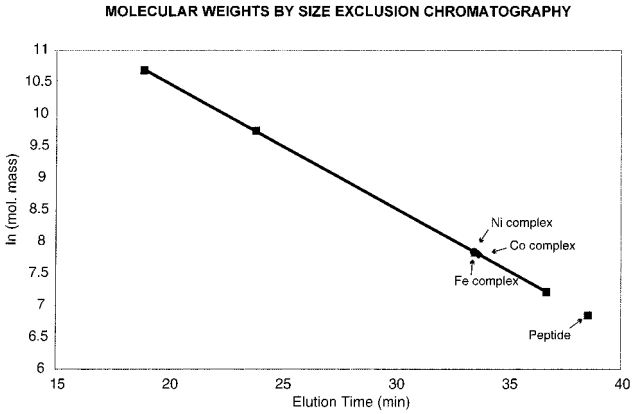

Figure 3. Calibration curve and experimental results for the determination of molecular weights of the cyclic peptide and its M(II) complexes by size exclusion chromatography in aqueous buffer at pH 7.5.

Molecular Weights. The cyclic peptide and its three metal complexes were subjected to size exclusion chromatography in order to estimate molecular weights. Separations were performed with a Rainin Dynamax instrument equipped with a Pharmacia Biotech Superdex 75 10/30 size exclusion column (300 × 10 mm). Buffer solutions were rigorously deoxygenated and maintained under positive helium pressure during the experiments. Isocratic separations were carried out with 20 mM Hepes buffer at pH 7.5 containing 50 mM NaCl and 2 mM $Na_2S_2O_4$ employing a flow rate of 0.5 mL/min and spectrophotometric monitoring at 355 nm. Solutions of complexes in the preceding medium were prepared under a dinitrogen atmosphere and injected via a gastight syringe. Molecular weights were estimated from the calibration plot in Figure 3 utilizing standards obtained from Bio Rad Laboratories. Cyclic peptide: calculated, 1193; found, 940. M(II) peptides: calculated, 1248−1250; found, 2500.

X-ray Absorption Spectroscopy. Under anaerobic conditions, lyophilized metallopeptide samples were loaded into 1 mm Lucite cells with 63.5 μM Kapton windows. Samples were frozen in liquid nitrogen immediately after preparation and were maintained at 77 K or a lower temperature throughout storage and data collection.

(a) Data Collection. XAS data were measured at the Stanford Synchrotron Radiation Laboratory (SSRL) on unfocused beamline 7-3 under ring conditions 3.0 GeV, 70−100 mA. A Si(220) double-crystal monochromator was utilized for energy selection at the Co and Ni K-edges. The monochromator was detuned 50% at 8831 eV (Co K-edge) and 9439 eV (Ni K-edge) to minimize contamination from higher harmonics. An Oxford Instruments CF1208 continuous flow liquid helium cryostat was used to maintain a constant sample temperature of 10 K. Data were measured in the fluorescence mode using a 13-element Ge array detector[39] to $k = 17$ Å^{-1} (Co K-edge) and $k = 16$ Å^{-1} (Ni K-edge). Internal calibration was performed by simultaneous measurement of absorption edges of a cobalt or nickel foil placed between a second and third nitrogen-filled ionization chamber. The first inflection point of the cobalt foil spectrum and nickel foil spectrum was assigned to 7709.5 and 8331.6 eV, respectively. The data represent averages of 12 and 20 scans for the cobalt and nickel peptides, respectively, with data reduction as described previously in detail.[40]

(38) Atherton, D. In *Techniques in Protein Chemistry*; Hugli, T. E., Ed.; Academic Press: New York, 1989; pp 273−283.

(39) Cramer, S. P.; Tench, O.; Yocum, M.; George, G. N. *Nucl. Instr. Methods A* **1988**, *266*, 586.

(b) Data Analysis. The data analysis was performed using the ab initio GNXAS method.[41−43] The program code generates theoretical EXAFS signals based on an initial structural model. For the analysis reported here, Cartesian coordinates for assumed cobalt and nickel coordinations (generated using Chem3D Pro) were used as input to generate an initial structural model up to a distance cutoff of 5.0 Å. Phase shifts were calculated using the standard muffin-tin approximation in order to calculate individual two-body EXAFS signals. A model EXAFS spectrum was constructed by combining individual component signals and an appropriate background. This theoretical model signal was then fit to the averaged raw absorption data by a least-squares minimization program that uses the MINUIT subroutine of the CERN library. Background subtraction was performed by applying a flexible three-segment spline which was refined in the GNXAS fits. The quality of the fit was calculated by the least-squares residual and monitored through visual inspection of fits to the data, Fourier transforms, and the residual EXAFS signal and its Fourier transform. The structural parameters varied during the refinements were the bond distance (R) and the bond variance (σ_R^2), related to the Debye−Waller factor, which is a measure of the thermal vibration and the static disorder of the absorber/scatterer.[43] The nonstructural parameters E_o (which aligns the ionization threshold of the theoretical signal to that of the experimental signal) and S_o^2 (the many-body amplitude reduction factor) were varied, whereas Γ_C (core hole lifetime), and E_r (experimental resolution) parameters were kept fixed to physically reasonable values throughout the analysis. The coordination numbers were systematically varied through the analysis but were not allowed to vary in a given fit. All parameters were varied within a preset range, and all results were checked to ensure that values obtained did not reach the high or low point of these fitting ranges.

Results and Discussion

Peptide Design and Synthesis. To identify possible metal-binding cyclopeptide targets, QUANTA molecular modeling was performed. Our considerations have focused on cyclopeptides because suitable design aspects might allow intramolecular metal binding or limit the extent of polynuclear complex formation and, possibly, promote crystallinity. Tetracysteinyl cyclopeptides with 10−12 residues (10−12mers) and two Cys−$(X)_n$−Cys (n = 1, 2) linkages between two linear fragments were found to be potentially amenable to mononuclear M(S·Cys)$_4$ coordination units of variable geometry. Smaller rings resulted in more constrained and exposed metal sites, with the attendant possibility of extensive polynuclear complex formation. The sequence run Cys−X−X−Cys is a frequently encountered element in metalloproteins. In our final model, we have selected the sequences Cys-Gly-Val-Cys and Cys-Ile-Ala-Cys which form the two chelate rings at the nickel site of *Desulfovibrio gigas* hydrogenase.[21] Synthetic iteration led to the 12mer cyclo-[Lys^{1,12}](Gln-Cys-Gly-Val-Cys-Gly-Lys-Cys-Ile-Ala-Cys-Lys) for our initial examination of potential M(S·Cys)$_4$ coordination.

In the synthetic procedure, Asp was initially introduced into the sequence as a part of the cyclization strategy. Unless this residue is at the C-terminus, aspartamide formation was found to be unavoidable. Aspartate was replaced by Glu, which is converted to Gln during resin cleavage. To facilitate cyclization further,[44] two Gly residues were placed at internal positions. Of the different Cys protection schemes explored, trityl, S−*tert*-butyl, and acetamidomethyl, only the latter was found to be suitable. Two Lys residues were incorporated to ensure aqueous solubility of the otherwise hydrophobic peptide. Synthesis of ⊂L(Cys·SH)$_4$ is summarized in Figure 1. Peptide identification and demonstration of purity are given in Figure 2. Preparations are homogeneous by HPLC, and the $(M + 2H)^+/2$ parent ion of the fully reduced peptide with the correct isotope distribution is observed. The peptide is quite stable when stored anaerobically at −20 °C; in aqueous solution in the presence of air, it is rapidly oxidized.

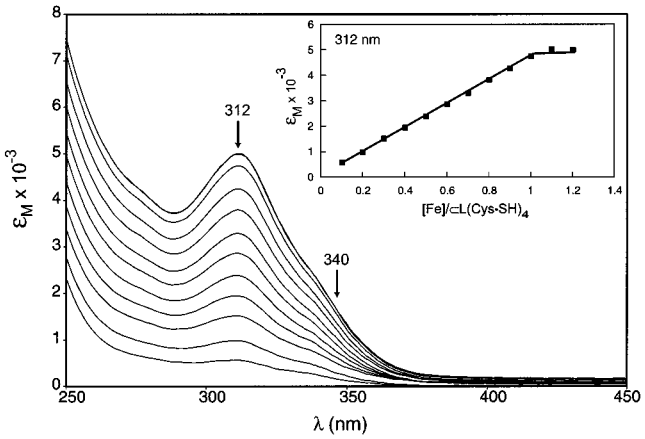

Figure 4. Spectrophotometric monitoring of the binding of Fe^{2+} by ⊂L(Cys·SH)$_4$ at pH 7.5. The inset shows 1:1 binding by following the absorption at 312 nm.

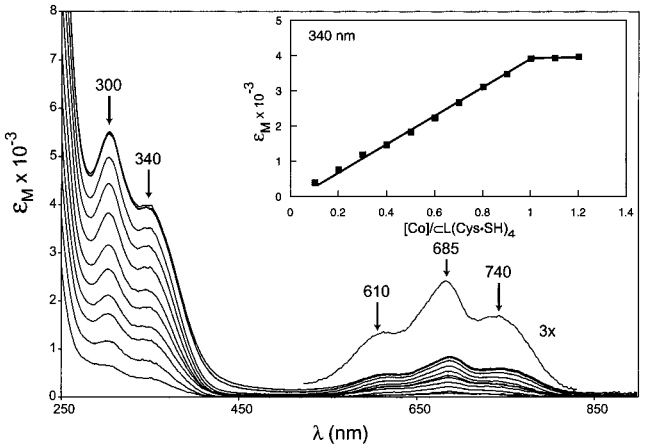

Figure 5. Spectrophotometric monitoring of the binding of Co^{2+} by ⊂L(Cys·SH)$_4$ at pH 7.5. The visible region is plotted at $3\epsilon_M$. The inset shows 1:1 binding by following the absorption at 340 nm.

Metal Binding. Binding interactions of three divalent metal ions with the cyclopeptide have been monitored spectrophotometrically as shown in Figures 4−6. Titrations reveal complete binding at a 1:1 metal−peptide stoichiometry. Band maxima and extinction coefficients of limiting spectra, together with appropriate comparison data for proteins and synthetic complexes, are collected in Table 1.

Reaction with Fe^{2+} yields a nearly colorless solution which exhibits two LMCT bands: an intense feature at 310 nm and a weaker shoulder at 340 nm. The final spectrum (Figure 4) compares closely with those of reduced rubredoxin[45] and [Fe(S$_2$-*o*-xyl)$_2$]$^{2-}$,[46] which are tetrahedral. Reaction with Co^{2+}

(40) DeWitt, J. G.; Bentsen, J. G.; Rosenzweig, A. C.; Hedman, B.; Green, J.; Pilkington, S.; Papaefthymiou, G. C.; Dalton, H.; Hodgson, K. O.; Lippard, S. J. *J. Am. Chem. Soc.* **1991**, *113*, 9219.
(41) Filipponi, A.; Di Cicco, A.; Tyson, T. A.; Natoli, C. R. *Solid State Commun.* **1991**, *78*, 265.
(42) Westre, T. E.; Di Cicco, A.; Filipponi, A.; Natoli, C. R.; Hedman, B.; Solomon, E. I.; Hodgson, K. O. *J. Am. Chem. Soc.* **1995**, *117*, 1566.
(43) Filipponi, A.; Di Cicco, A.; Natoli, C. R. *Phys. Rev. B* **1995**, *52*, 15122, 15135.
(44) Cavelier-Frontin, F.; Pèpe, G.; Verducci, J.; Siri, D.; Jacquier, R. *J. Am. Chem. Soc.* **1992**, *114*, 8885.
(45) Lovenberg, W.; Sobel, B. E. *Proc. Natl. Acad. Sci. U.S.A.* **1965**, *54*, 193.

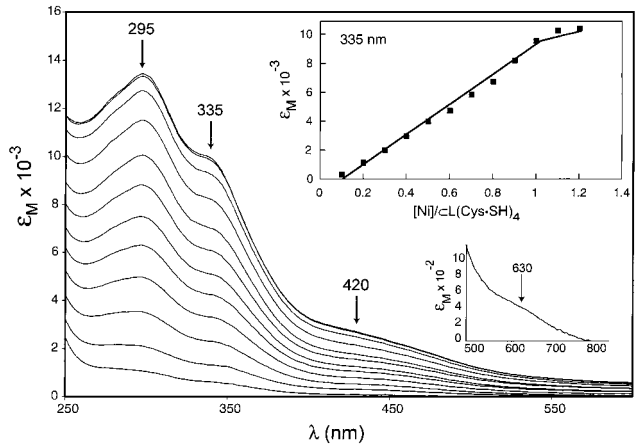

Figure 6. Spectrophotometric monitoring of the binding of Ni^{2+} by ⊂L(Cys·SH)$_4$ at pH 7.5. The inset shows 1:1 binding by following the absorption at 335 nm.

generates a greenish solution whose spectrum shows LMCT bands at 300 and 340 nm (Figure 5). The latter features find counterparts in the spectra of Co^{II} rubredoxin,[47] $[Co(S_2\text{-}o\text{-}xyl)_2]^{2-}$,[46] mono- and polynuclear cobalt(II) thiolates,[48] and a Co(II) complex of a tetracysteinyl linear 26mer peptide.[49] The visible region consists of features at 610, 685, and 740 nm which are unmistakably those of a tetrahedral $Co^{II}(SR)_4$ chromophore.[46] These bands are components of the parent tetrahedral ligand field transition $^4A_2 \rightarrow {}^4T_1(P)$ split by lower symmetry. Reaction with Ni^{2+} generates a light brownish solution with a LMCT band at 335 nm and probable d−d features at 420 and 630 nm (Figure 6). This spectrum bears a clear relationship to those of planar complexes $[Ni_2(S_2\text{-}o\text{-}xyl)_3]^{2-}$[46] and $[Ni(S_2\text{-}norbornane)_2]^{2-}$.[30] It is unrelated to those of Ni(II) rubredoxin[32] and $[Ni(SPh)_4]^{2-}$, which are tetrahedral. The complex $[Ni_2(S_2\text{-}o\text{-}xyl)_3]^{2-}$ is a particularly clear example of the tendency for Ni(II) alkylthiolates to form polynuclear species. Despite numerous attempts in this laboratory, including those with large excesses of ligand, we have never been able to isolate mononuclear $[Ni(S_2\text{-}o\text{-}xyl)_2]^{2-}$, which we anticipate to be planar. Related experiments by others have also not resulted in the mononuclear complex, and in addition have afforded trinuclear $[Ni_3(S_2\text{-}o\text{-}xyl)_4]^{2-}$.[20,50,51]

The absorption spectral results support the solution stereochemical assignments of tetrahedral for the Fe(II) and Co(II) complexes and planar for the Ni(II) complex. They do not address the molecularity of the complexes, which was investigated by size exclusion chromatography. Under solution conditions similar to those used in the spectrophotometric titrations, but with the inclusion of sodium dithionite to scavenge dioxygen, this method indicates that the three complexes are dimers $[M_2(\subset L(Cys\cdot S)_4)_2]$. Possible dimeric structures are considered subsequently. Solution molecular weights are infrequently reported for cysteinyl peptide complexes. To examine streochemical assignments in the solid state and obtain further structural information, we have examined lyophilized samples of the Co(II) and Ni(II) complexes by XAS.

XAS Results. (a) Edges. The cobalt K-edge data are shown in Figure 7 (upper). An intense preedge feature is seen at 7709 eV. This feature is assigned as a formally dipole-forbidden 1s → 3d transition, which derives intensity mainly from electric-dipole 3d−4p mixing and, to a small extent, from electric quadrupole coupling.[52−54] A high degree of 3d−4p mixing occurs in noncentrosymmetric molecules, particularly with tetrahedral geometry. Thus, the high intensity of the preedge absorption strongly indicates a tetrahedral structure.

The nickel K-edge results are presented in Figure 7 (lower). Extensive XAS studies have identified and interpreted the systematic relationship between nickel K-edge structure and electronic/geometric configuration.[55−58] The lack of an intense preedge feature of the sort seen for the Co(II) peptide indicates that the Ni(S·Cys)$_4$ unit approaches a centrosymmetric microsymmetry such as square planar or octahedral, both of which have very small preedge transitions (if they are seen at all). It has also been shown that complexes approaching square planar geometry exhibit a spike in the rising edge at ∼8337 eV, which has been assigned as a 1s → $4p_z$ or 1s → 4p plus shakedown transition and which decreases in intensity upon distortion from ideal symmetry.[55−58] This situation is illustrated in Figure 8, where edge structure is correlated with stereochemistry. The square planar reference is $(Bu_4N)_2[Ni(S_2C_2(CN)_2)_2]$,[59] in which the anion is centrosymmetric with Ni−S bond distances of 2.173(1) and 2.176(1) Å and a S−Ni−S bite angle of 92.2(1)°. The distorted square planar reference is the classic binuclear complex $[Ni_2(\mu\text{-}SCH_2CH_2SCH_2CH_2S)_2]$,[60,61] of idealized C_2 symmetry. In the crystalline state, the molecule contains two slightly inequivalent NiS_4 units with terminal thiolate and thioether sulfur ligands and two bridging thiolates. The Ni−S bond lengths are 2.152(5)−2.217(5) Å and S−Ni−S angles are 82.6(2)−96.7(2)°. The nickel atoms are displaced by 0.1 Å from their S_4 planes.[61] The tetrahedral reference is $(Ph_4P)_2[Ni(SPh)_4]$,[24,25] but in terms of angular parameters the complex actually is severely distorted from T_d microsymmetry. Two of the S−Ni−S angles are near 90° and the other four are in the 109−125° range; bond distances average to 2.29(1) Å. From a comparison of the edges, it is clear that the Ni(II) peptide closely resembles the distorted square planar species, a conclusion consistent with the assignment of a planar structure from the absorption spectrum.

(b) EXAFS Analysis. The EXAFS data for the Co(II) and Ni(II) peptides, presented in Figure 9, consist of one single-frequency, regular wave for each complex, indicating one type of ligand at about the same distance from the metals. This is further supported by the Fourier transform (not shown), which contains only one intense peak at ∼1.95 and 1.85 Å (nonphase-

(46) Lane, R. W.; Ibers, J. A.; Frankel, R. B.; Papaefthymiou, G. C.; Holm, R. H. *J. Am. Chem. Soc.* **1977**, *99*, 84.
(47) May, S. W.; Kuo, J.-Y. *Biochemistry* **1978**, *17*, 3333.
(48) Hagen, K. S.; Holm, R. H. *Inorg. Chem.* **1984**, *23*, 418.
(49) Krizek, B. A.; Merkle, D. L.; Berg, J. M. *J. Am. Chem. Soc.* **1993**, *32*, 937.
(50) Tremel, W.; Krebs, B.; Henkel, G. *Angew. Chem., Int. Ed. Engl.* **1984**, *96*, 604.
(51) Tremel, W.; Kriege, M.; Krebs, B. *Inorg. Chem.* **1988**, *27*, 3886.
(52) Shulman, R. G.; Yafet, Y.; Eisenberger, P.; Blumberg, W. E. *Proc. Natl. Acad. Sci. U.S.A.* **1976**, *73*, 1284.
(53) Bair, R. A.; Goddard, W. A. *Phys. Rev.* **1980**, *B22*, 2767.
(54) Westre, T. E.; Kennepohl, P.; DeWitt, J. G.; Hedman, B.; Hodgson, K. O.; Solomon, E. I. *J. Am. Chem. Soc.* **1997**, *119*, 6297.
(55) Eidsness, M. K.; Sullivan, R. J.; Scott, R. A. In *The Bioinorganic Chemistry of Nickel*; Lancaster, J. R., Jr., Ed.; VCH: New York, 1988, Chapter 4.
(56) Cramer, S. P. Eidsness, M. K.; Pan, W. H.; Morton, T. A.; Ragsdale, S. W.; DerVartanian, D. V.; Ljungdahl, L. G.; Scott, R. A. *Inorg. Chem.* **1987**, *26*, 2477.
(57) Colpas, G. J.; Maroney, M. J.; Bagyinka, C.; Kumar, M.; Willis, W. S.; Suib, S. L.; Baidya, N.; Mascharak, P. K. *Inorg. Chem.* **1991**, *30*, 920.
(58) Maroney, M. J.; Colpas, G. J.; Bagyinka, C.; Baidya, N.; Mascharak, P. K. *J. Am. Chem. Soc.* **1991**, *113*, 3962.
(59) Kobayashi, A.; Sasaki, Y. *Bull. Chem. Soc. Jpn.* **1977**, *50*, 2650.
(60) Baker, D. J.; Goodall, D. C.; Moss, D. S. *Chem. Commun.* **1969**, 325.
(61) Barclay, G. A.; McPartlin, E. M.; Stephenson, N. C. *Acta Crystallogr.* **1969**, *B25*, 1262.

Table 1. Absorption Spectral Data

species	λ_{max} (ϵ_M)[a]	ref
$[Fe_2(\subset L(Cys\cdot S)_4)_2]$	310 (5030), 340 (sh, 2320)	*b*
Fe^{II} rubredoxin	311 (10,800), 333 (6300)	45
$[Fe(S_2\text{-}o\text{-}xyl)_2]^{2-}$	322 (7410), 355 (sh, 3070)	46
$[Co_2(\subset L(Cys\cdot S)_4)_2]$	300 (5430), 340 (sh, 3920), 610 (470), 685 (840), 740 (570)	*b*
Co^{II} rubredoxin	350 (9400), 470 (3010), 620 (1130), 685 (1230), 748 (1030)	47
$[Co(S_2\text{-}o\text{-}xyl)_2]^{2-}$	355 (3450), 610 (481), 684 (645), 788 (460)	46
$[Ni_2(\subset L(Cys\cdot S)_4)_2]$	335 (9400), 420 (sh, 2630), 630 (sh, 435)	*b*
$[Ni_2(S_2\text{-}o\text{-}xyl)_3]^{2-}$	486 (1880), 620 (sh, 262)	46
$[Ni(S_2\text{-norbornane})_2]^{2-}$	388 (sh, 549), 460 (307), 633 (118)	30
Ni^{II} rubredoxin	360 (5460), 450 (3200), 670 (385), 720 (460)	32

[a] Units: nm (M^{-1} cm^{-1}); ϵ_M per metal atom. [b] This work.

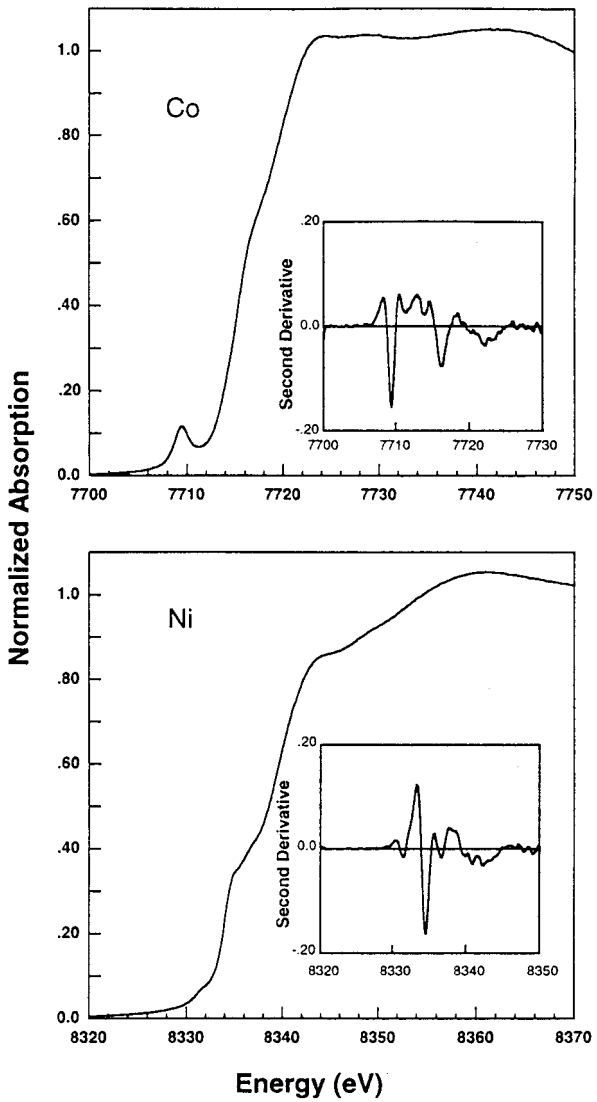

Figure 7. Normalized cobalt and nickel K-edge spectra of the Co(II) (upper) and Ni(II) (lower) peptides with the corresponding second derivative spectra shown as insets. Significant differences are seen in the preedge region and the rising edge.

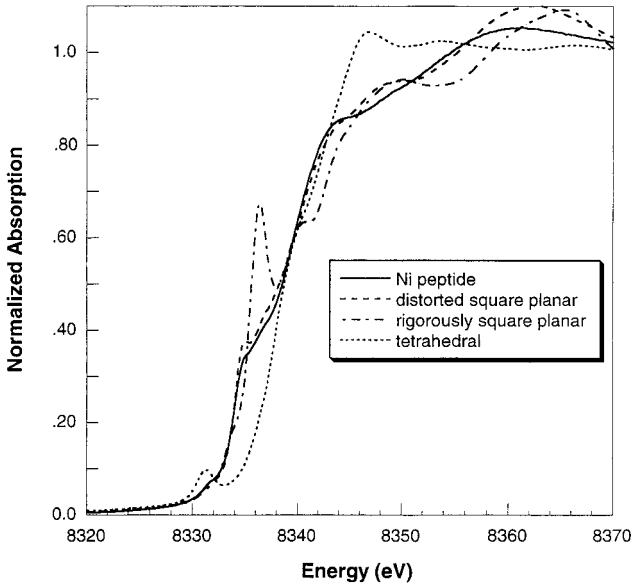

Figure 8. Normalized nickel K-edge spectra of the Ni(II) peptide (—), planar $[Ni(S_2C_2(CN)_2)_2]^{2-}$ as the Bu_4N^+ salt (— · —), distorted square planar $[Ni_2(\mu\text{-}SCH_2CH_2SCH_2CH_2S)_2]$ (- - -), and tetrahedral $[Ni(SPh)_4]^{2-}$ as the Ph_4P^+ salt (···). The edge of the Ni(II) peptide is seen to correlate best with that of the distorted planar complex.

shift corrected) for the Co(II) and Ni(II) peptides, respectively. The shape of the amplitude envelope of the EXAFS wave is indicative of sulfur ligation. The best fits to the data (Figure 9) were obtained for a coordination number of four for the M−S interaction, giving distances of 2.30 and 2.21 Å, and bond variance parameters of 0.0019 and 0.0017 $Å^2$ for the Co(II) and Ni(II) peptides, respectively. EXAFS fit results are summarized in Table 2. Attempted fits with coordination numbers higher than four resulted in visually poor fits to the data, unreasonably low bond variance parameters (0.0001−0.0006 $Å^2$), and higher R values. The cobalt and nickel EXAFS data have a very similar appearance; however, the nickel data is frequency-shifted relative to the cobalt data, which is consistent with the shorter Ni−S distance determined. A coordination number of four is in agreement with the edge analysis. The Co−S distance is central to the range of mean values of terminal bond lengths (2.26−2.33 Å) in the tetrahedral sites of $[Co(SPh)_4]^{2-}$,[25] *syn*- and *anti*-$[Co_2(SEt)_6]^{2-}$,[48] $[Co_2(S_2\text{-}o\text{-}xyl)_3]^{2-}$,[62] and $[Co_4(SPh)_{10}]^{2-}$,[63] all of which show different distortion patterns from T_d microsymmetry. The Ni−S bond length of 2.21 Å is entirely compatible with a large body of structural data for the planar $Ni^{II}S_4$ unit, including the bis(dithiolato) complexes $[Ni(SCH_2CH_2S)_2]^{2-}$ (2.195 Å)[29] and $[Ni(S_2\text{-norbornane})_2]^{2-}$ (2.184 Å).[30] It is incompatible with the tetrahedral value of 2.29 Å for $[Ni(SPh)_4]^{2-}$.[25]

Binuclear Structures. Many different binding modes of two metals to eight (or six) cysteinyl sulfur atoms of the two cyclic peptides can be conceived. Assuming a nonbridged structure with all eight cysteinyl residues coordinated, the question arises as to which four are bound to a given metal center. We favor an arrangement in which two residues from each peptide bind

(62) Tremel, W.; Krebs, B.; Henkel, G. *Angew. Chem., Int. Ed. Engl.* **1984**, *23*, 634.
(63) Dance, I. G. *J. Am. Chem. Soc.* **1979**, *101*, 6264.

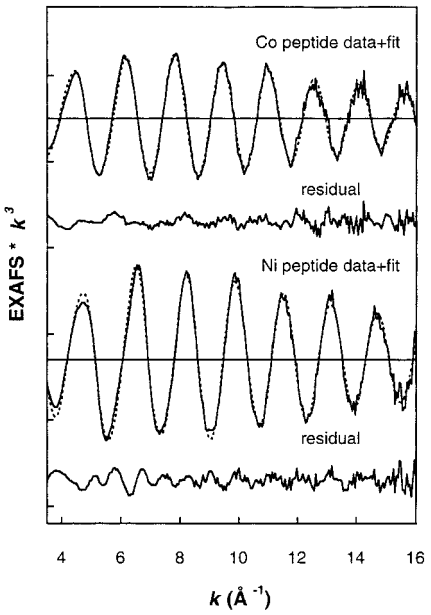

Figure 9. Comparison of the experimental EXAFS data (—) and fits to the data (- - -) for the Co(II) peptide (upper) and the Ni(II) peptide (lower). (The ordinate is 10 units below each tick mark.)

Table 2. Co and Ni K-Edge EXAFS Analysis Fit Results[a]

	[Co(⊂L(Cys·S)$_4$)]	[Ni(⊂L(Cys·S)$_4$)]
E_o	7721.9	8341.8
S_0^2	0.80	0.84
R(M−S) (Å)	2.30	2.21
N[a]	4	4
σ^2 (Å^2)	0.0019	0.0017
×c2(fit)	0.795×10^{-7}	0.116×10^{-6}

[a] In the fits, the following parameters were refined: E_o, S_0^2, R, and the corresponding σ^2 values. The coordination numbers (N) were systematically varied through the analysis but were not allowed to vary in a given fit. The Γ_o and experimental resolution parameters were fixed to physically reasonable values through the analysis. Estimated standard deviations for the distances are on the order of ±(0.01−0.02) Å.

to the same metal. With reference to the Cys residue numbering scheme in Figure 1, we have examined in particular the binding patterns M(1/2,5/6-Cys·S)$_4$ + M(3/4,7/8-Cys·S)$_4$ for planar coordination and M(1/2,5/6-Cys·S)$_4$ + M(5/6,7/8-Cys·S)$_4$ for tetrahedral coordination. (Residue numbers 1−4 refer to one peptide and 5−8 to the other). Thereafter, the QUANTA software package was used to investigate possible peptide conformations in [M$_2$(⊂L(Cys·S)$_4$)$_2$] with the two coordination geometries. Positions of the metal and sulfur atoms were fixed and typical bond distances and angles were assigned. The structures were refined in CHARMM to ensure than no unreasonable close contacts or geometries were present. Conformations associated with planar and tetrahedral coordination are presented in Figure 10. It is not claimed that these structures represent global minima, only that they are plausible. These considerations do not address bridged structures of the type [M$_2$(μ-SR)$_2$(SR)$_4$]$^{2-}$, which are well established for M = Fe(II), Co(II), and Ni(II) with metal−metal separations of ca. 2.9−3.1 Å.[28,48,62] However, EXAFS results do not indicate the presence of metal−metal interactions in this range. If the structure in Figure 10 is correct, [Ni$_2$(⊂L(Cys·S)$_4$)$_2$] contains the first case of planar nonbridged Ni(II) tetrathiolate, albeit in a binuclear molecule.

Summary. The tetracysteinyl cyclopeptide ⊂L(Cys·SH)$_4$ has been synthesized by solid-phase methods using an Fmoc/*t*-Bu/allyl strategy on a PAL−PEG−PS support. The peptide binds

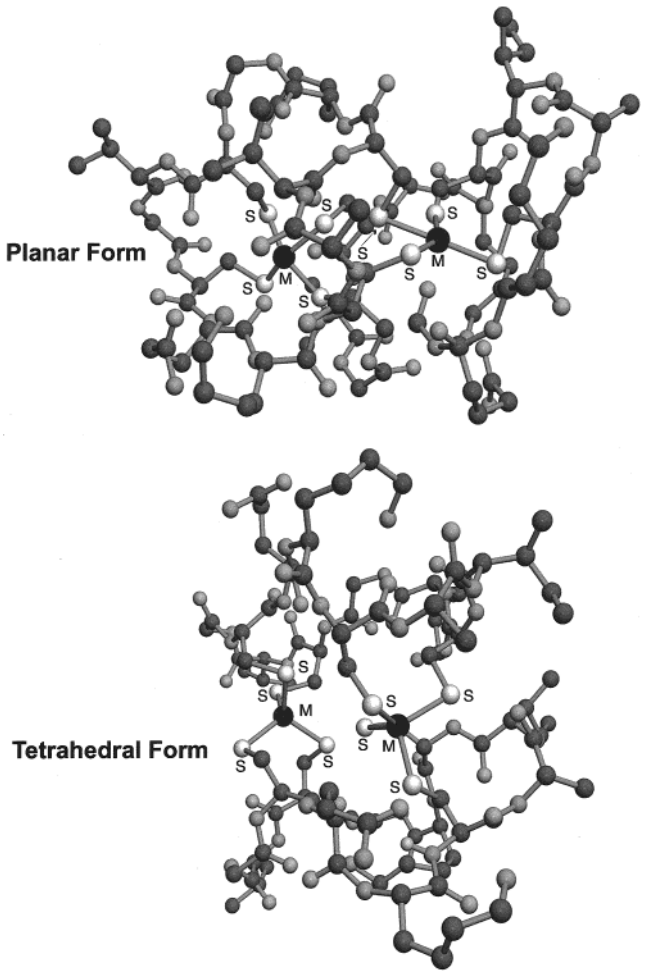

Figure 10. Possible structures for [Ni$_2$(⊂L(Cys·S)$_4$)$_2$] (upper) and [M$_2$(⊂L(Cys·S)$_4$)$_2$] (lower, M = Fe(II), Co(II)) based on two Cys residues from each peptide coordinated to a given metal center (see text) and peptide conformations refined in CHARMM.

Fe^{2+}, Co^{2+}, and Ni^{2+} in 1:1 complexes in aqueous solution at pH 7.5. From the collective evidence provided by absorption spectra, cobalt and nickel K-edge data, and EXAFS analysis and bond length comparisons with known structures, the Fe(II) and Co(II) peptides are shown to possess distorted tetrahedral and the Ni(II) peptide a distorted planar structure. In the medium 20 mM HEPES buffer/50 mM NaCl/pH 7.5, the results from size exclusion chromatography are consistent with a monomeric cyclopeptide and dimeric [M$_2$(⊂L(Cys·S)$_4$)$_2$] complexes (in the presence of 2 mM sodium dithionite). We have no information on molecularity in the solid state. Plausible binuclear structures can be constructed, among them the representations in Figure 10. The dimeric nature of the metal(II) peptide complexes raises the possibility of bridged or cross-linked structures for other metallocysteinylpeptides of unknown molecular weight. These are among the first characterized complexes of a synthetic cysteinyl cyclopeptide and are among the few well-documented complexes of cyclopeptides in general. This work is the initial step in the problem of designing and synthesizing cyclic peptides for binding of metal ions and clusters of biological significance.

Acknowledgment. This research was supported by Grants NIH GM 28856 and NSF CHE 95-23830 (to R.H.H) and NSF CHE 9423181 and NIH RR-01209 (to K.O.H). The Stanford Synchrotron Radiation Laboratory is supported by the Department of Energy, Office of Basic Energy Sciences. The Bio-

technology Program is supported by the National Institutes of Health, National Center for Research Resources, Biomedical Technology Program and by the DOE Office of Biological and Environmental Research. The data for $(Ph_4P)_2[Ni(SPh)_4]$ and $(Bu_4N)_2[Ni(S_2C_2(CN)_2)_2]$ were kindly provided by Prof. R. A. Scott, University of Georgia. We are grateful to Dr. Juan C. Fontecilla-Camps for providing the X-ray coordinates of *D. gigas* hydrogenase.

IC990421L